Design of compliant joints for large scale structures

Nastevska, Angela; Jovanova, Jovana; Frecker, Mary

Citation (APA)
Nastevska, A., Jovanova, J., & Frecker, M. (2020). Design of compliant joints for large scale structures. In *Proceedigs of the ASME Conference on Smart Materials, Adaptive Structures and Intelligent Systems, SMASIS 2020* Article V001T06A007 ASME. https://doi.org/10.1115/SMASIS2020-2348

Important note
To cite this publication, please use the final published version (if applicable).
Please check the document version above.

SMASIS2020-18096

DESIGN OF COMPLIANT JOINTS FOR LARGE SCALE STRUCTURES

Angela Nastevska
Student
Faculty of Mechanical Engineering
Ss Cyril and Methodius University in Skopje
Skopje, Republic of North Macedonia

Jovana Jovanova
Assistant professor
Mechanical, Maritime and Materials Engineering
Delft University of Technology
Delft, Netherlands

Mary Frecker
Professor
Dept. of Mechanical Engineering
The Pennsylvania State University
University Park, PA, USA

ABSTRACT

Large scale structures can benefit from the design of compliant joints that can provide flexibility and adaptability. A high level of deformation is achieved locally with the design of flexures in compliant mechanisms. Additionally, by introducing contact-aided compliant mechanisms, nonlinear bending stiffness is achieved to make the joints flexible in one direction and stiff in the opposite one. All these concepts have been explored in small scale engineering design, but they have not been applied to large scale structures. In this paper the design of a large scale compliant mechanism is proposed for novel design of a foldable shipping container. The superelasticity of nickel titanium is shown to be beneficial in designing the joints of the compliant mechanism.

Keywords: large scale design, nitinol, contact aided compliant arrays, metamaterials.

NOMENCLATURE

E_A Modulus of elasticity of austenite phase
E_t Modulus of elasticity of martensite transformation
σ_s^{AS} Critical transformational stress of the NiTi material
σ_f^{AS} Final stress value for the forward phase transformation
φ Folding angle of the compliant joint

1. INTRODUCTION

Large scale design is mainly associated with maritime, aerospace, transportation, and civil engineering, when at least one of the geometric features is measured in meters. Typical megastructures include cargo containers, airplane wings, windmills, cranes, and other machinery used in ports. In order to explore smart concepts such as modularity, multifunctionality and foldability in large-scale structures novel design approaches are necessary. The concept of deployable structures has been explored in aerospace engineering [1 - 3], civil engineering [4, 5], and architecture [6], however smart design concepts in the maritime industry and in port equipment design are not as common. A general framework for design and optimization of self-folding structures is presented in [7]. The mechanical advantage of folding mechanism based on origami is modelled as a multi-input compliant mechanism in [8].

One way to achieve global shape change of a structure is by introducing large local deformations with the design of compliant joints [9]. High local compliance can be achieved with the design of flexures, taking advantage of the combined effort of the geometry and material for controlled overall shape change [10, 11]. To explore shape and stiffness tailorability, the concept

of contact-aided compliant mechanisms [12 - 14] is proposed where nonlinear bending stiffness makes the joints flexible only in one direction and stiff in the opposite one. All previously mentioned design concepts have been explored in small scale engineering design, but they have not yet been applied in the large scale domain. Design optimization, smart material integration and design for additive manufacturing (DfAM) can bring benefits to the design of innovative flexible and adaptable megastructures.

In this paper the design of large scale compliant mechanisms is proposed for novel design of a foldable shipping container. Steel and Nickel Titanium alloy (Nitinol) are explored as material options. Thesuperelastic behavior of Nitinol can provide large recoverable strains and low stresses in the compliant joint design. The superelasticity can be additionally tailored if additive manufacturing is used as fabrication approach. The operational temperatures are assumed to be lower than the shape memory transition temperature, so in the design analyses temperature is not considered. However, the shape memory effect can be further explored for actuation of the compliant joints. Different compliant joints are modelled and analyzed including contact-aided compliant arrays and metamaterials. The paper is structured as follows: Section 1 describes the design objectives; Section 2 is focused on the contact-aided compliant mechanism and contact-aided compliant arrays are analyzed for mechanism performance; In Section 3 a metamaterial design of the compliant joint is presented; and Section 4 shows comparative analyses. Finally there is a summary of the conclusions and potential for future work.

2. DESIGN OBJECTIVES

Standardized shipping containers that are mostly used in the transport industry have not had many improvements since the beginning when they revolutionized container shipping. The cost of shipping empty containers has been recognized and initiated designs for collapsible containers that have two stable positions, operational, and fully collapsed for transport [15,16]. However, with the rise of e-commerce the parcels become smaller and the customers expect lower time to market. Shipping containers need to be adapted to modern needs. One way is to design reconfigurable shipping containers which would make them adjustable to different quantities and parcel sizes.

In this paper a novel design of the sides of a reconfigurable shipping container with compliant joints is proposed to enable controllable folding. The superelasticity of NiTi can be beneficial in designing the compliant jointw due to the high flexibility of the material. These compliant superelastic joints may be added to the standardized containers' designs, making

them reconfigurable based on the current demand. Furthermore the superelastic joints can be externally electrically actuated to take advantage of the shape memory effect of NiTi, allowing stiff and flexible state configurations of the container.

Another way of achieving local compliance is with metamaterial flexures benefiting from the geometrical distribution of the compliant joints. Design for additive manufacturing (DfAM) could lead to an exploration of different 3D shapes and local material spatial distribution for achieving the desired global shape change.

In this work we analyze the side wall of a standard shipping container. The wall is modelled as two rigid panels with a flexible compliant joint shown in blue in Figure 1. The objective is to design a compliant joint that can perform a complete 180 degree fold shown in Figure 1 without exceeding a stress constraint.
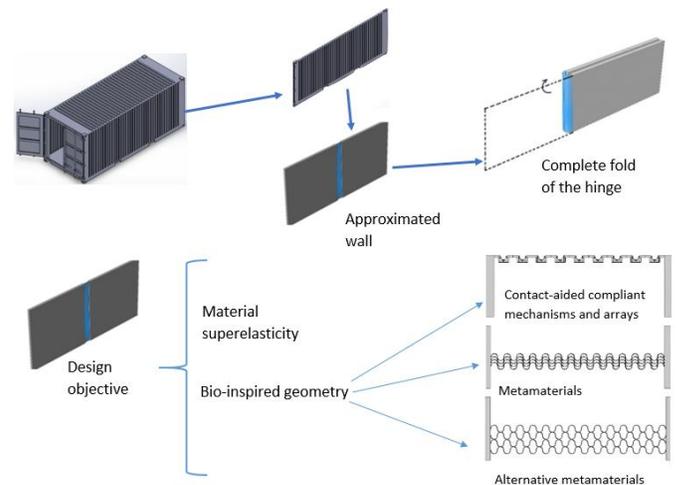

FIGURE 1: DESIGN OF A FOLDABLE SIDE WALL OF A CARGO CONTAINER BY INTRODUCING A COMPLIANT JOINT

Different geometric and mechanical property design concepts are proposed and analyzed for performance. The compliant joint designs are based on a compliant arc lattice as pictured in Figure 2. Lattices are bio-inspired structures commonly found in nature like a honeycomb structure. From the arc a contact-aided compliant unit cell has been designed and multiplied in an array. Then using the same compliant arc, series of metamaterial designs were developed. As for the materials used in the designs, two metals have been considered, AISI 4340 steel and superelastic NiTi. The dimensions of the cross section of the side wall of the container are shown in Figure 2 (a). The side walls that are connected by the hinge are 1 m long and have width of 36 mm. This is the width of the corrugated sheet metal used on the side walls of standard shipping containers. The

length of the hinge is assumed to be 10% of the length of the side walls that it connects. The entire structure is considered to have a depth of 1m. The targeted shape (complete fold) of the joint is shown in Figure 2. A complete fold is achieved when the free rigid panel of the structure has rotated φ=π radians or 180 degrees, i.e., when the free wall is on top of the fixed wall.
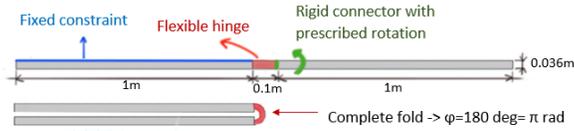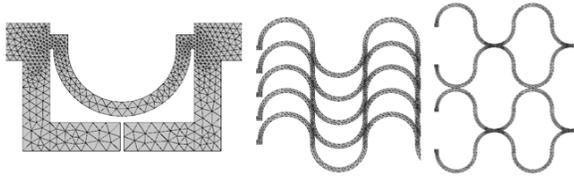
FIGURE 2: MODEL CONSTRAINTS: (a) CONSTRAINTS AND LOADS AND (b) MESH OF THE DIFFERENT GEOMETRIES

FEA analyses of all designs are done in COMSOL Multiphysics. For these analyses the structural mechanics module is used, and a quasi static study is performed. For the simulations the fully coupled solver is used. The model has relative tolerance of 0.001 and geometric nonlinearities are included. For reduced computational time, a 2D representation of the cross section shown in Figure 2 (a) is used. The approximation uses the plane strain condition, which does not allow expansion in the out-of-plane direction. The constraints and loads of the FEA model are shown in Figure 2 (a). The model is fixed in all directions on the left upper line marked in blue, which also disables deformation of the left wall. The model has prescribed rotation from 0 to π rad with a constant step size of π/50 rad. A prescribed rotation is set on the rigid connector at the end of the flexure marked in green. For all of the studies an automatic physics controlled mesh is used. The mesh has maximum element size of 21 mm, minimum element size of 0.042 mm, maximum element growth rate of 1.1, curvature factor of 0.2 and resolution of narrow regions of 1 and the geometry shape order is quadratic serendipity. The mesh for the different geometries is shown on Figure 2 (b).

The steel material is from the COMSOL material library with Young's modulus of 209 GPa, density of 7850 kg/m³ and Poisson's ratio of 0.28. On the other hand the Nitinol is modelled as a nonlinear material using the model shown in Figure 3 [17].
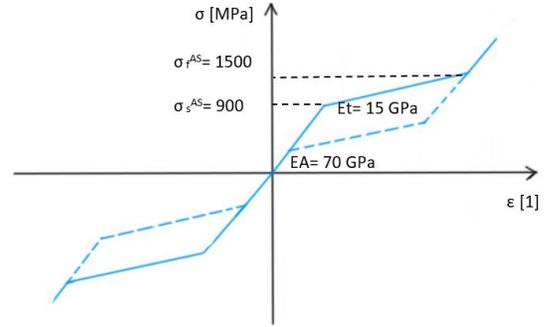

FIGURE 3: STRESS-STRAIN MATERIAL MODEL OF THE SUPERELASTIC NITI

The modulus in the austenite phase is set to be 70 GPa and in the martensite phase is 15 GPa. The starting stress value for the forward phase transformation is 900 MPa, and the final stress value for the forward phase transformation is 1500 MPa, therefore this value is chosen as a stress constraint to ensure that the behavior remains elastic. The values used in this model are based on data from [18, 19].

3. CONTACT-AIDED COMPLIANT MECHANISMS AND COMPLIANT ARRAYS

A contact-aided compliant mechanism with nonlinear stiffness is designed, as shown in Figure 4 (a). The mechanism is flexible in only one bending direction, marked blue in Figure 4 (a). In the opposite direction the mechanism has higher bending stiffness due to the contact surfaces marked in red.
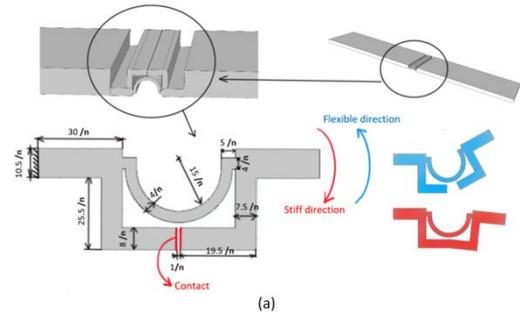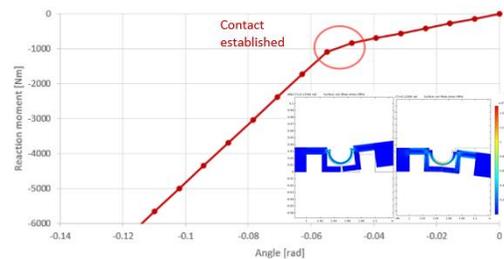
FIGURE 4: CONTACT-AIDED COMPLIANT MECHANISM

In Figure 4 (b) the reaction moment for corresponding input rotation angles is shown. It can be seen that when the contact is established in the compliant mechanism, the slope of this curve changes, i.e., the bending stiffness is nonlinear. The images in Figure 4 (b) show the Von Mises stress distributions in the mechanism in the two directions, the flexible (left) and the stiff (right).

The mechanism in Figure 4 is designed to fit within the area of the compliant joint in 2D marked in blue in Figure 2 which has length of 100 mm and width of 36mm. This means that in order to fit n-number of mechanisms in the same area, the mechanism geometry has to be scaled by a factor of 1/n. The dimensions are parametric where n is the number of cells placed in the hinge as shown in Figure 5.
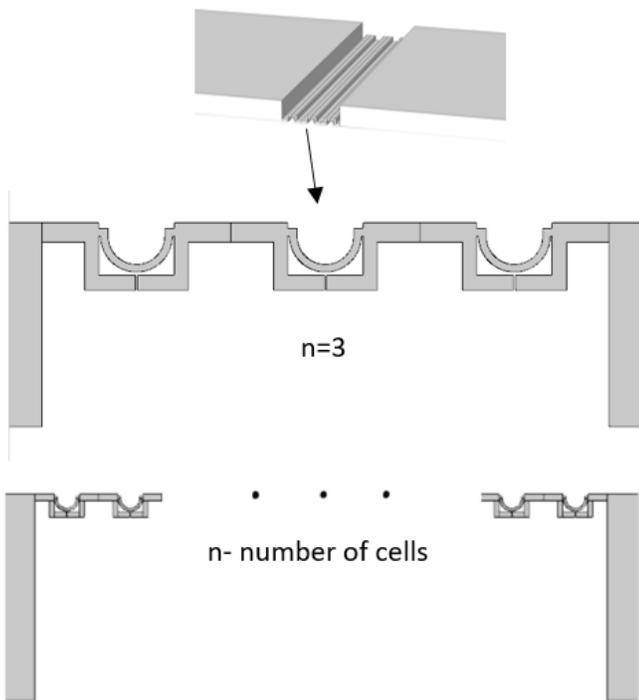

FIGURE 5: CONTACT-AIDED COMPLIANT ARRAYS WITH N-NUMBER OF CELLS

By making the cells smaller and combining a higher number of cells in the horizontal direction within the same area, compliant arrays are formed. In Figure 5 the compliant array with three cells is shown. As the dimensions of the cell are made smaller n-number of cells can fit in the same area. Additionally as shown in Figure 5 the compliant array is positioned at the top of the hinge area.

In the analysis, compliant arrays built with 1,3,5,7,9 and 13 cells are compared. The results of this comparison where the cells are made of the steel material are shown in Figure 6. For each compliant array, the reported stress is the maximum Von Mises stress of an arc measured always in the middle cell of the array. The higher number of cells results in lower stress for the same deformation of the hinge, or rotation of the wall. For the same stress constraint only the array made of 13 cells is able to achieve the complete fold of π radians. It is also important to note that by increasing the number of cells, the targeted fold is achieved even though a relatively stiff material like the steel is being used. One of the drawbacks of this design are the dimensions which are relatively small. For example, if the thickness of the arc when n=1 is 4mm the same dimension for n=13 is 0.3mm.
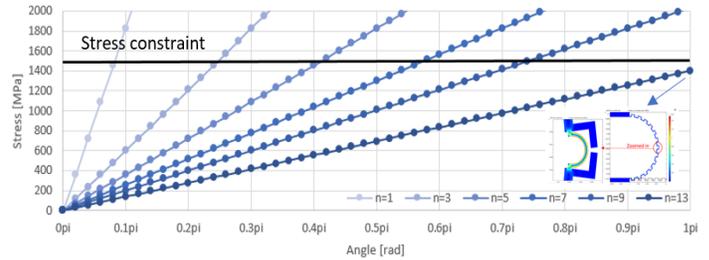

FIGURE 6: STRESS DISTRIBUTION. MAXIMUM VON MISES STRESS IN THE MIDDLE CELL OF THE ARRAY WITH STEEL AISI 4340. STRESS DISTRIBUTION AND DEFORMATION FOR THE STRUCTURE WITH 13 CELLS AT THE STRESS CONSTRAINT

In Figure 7 the maximum von Mises stress measured in the middle cell of the array made of Nitinol is shown. Even with this material the effect of the geometry and the higher number of cells has a similar impact in the performance of the structure. For the steel compliant arrays, only the array with 13 cells was able to achieve angle of π radians while staying bellow the stress constraint. On the contrary, when using Nitinol, only the compliant array made of one cell is not able to achieve the complete fold while satisfying the stress constraint. The benefit of the superelastic behavior of NiTi is illustrated by the case when n=1. The superelasticity increases the achieved angle of rotation by more than two times compared to the same stell design, and it rotates almost π/2 before reaching the stress constraint. This effect is even more notable for the case of n=3. With the superelastic behavior the structure achieves the targeted angle of rotation or the complete fold while satisfying the stress constraint. In Figure 7 the dotted line represents the stress level for the forward phase transformation which is 900 MPa. Since Nitinol is more flexible than the steel, it can be seen that even before the transition to superelasticityn (represented by the the dotted line) the performance of the arrays is better with Nitinol. The n=13 compliant array made with NiTi has around 3.5 times lower stress for the same rotation of π radians than the same steel design.
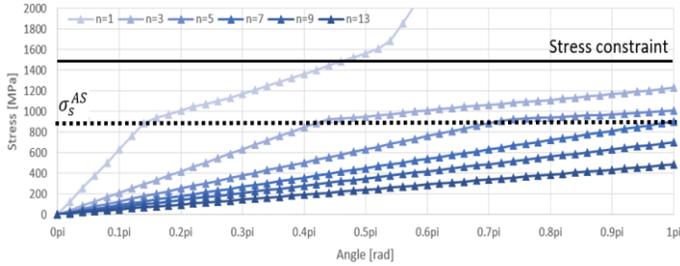
FIGURE 7: MAXIMUM VON MISES STRESS IN THE MIDDLE CELL OF THE ARRAY WITH NITI MATERIAL

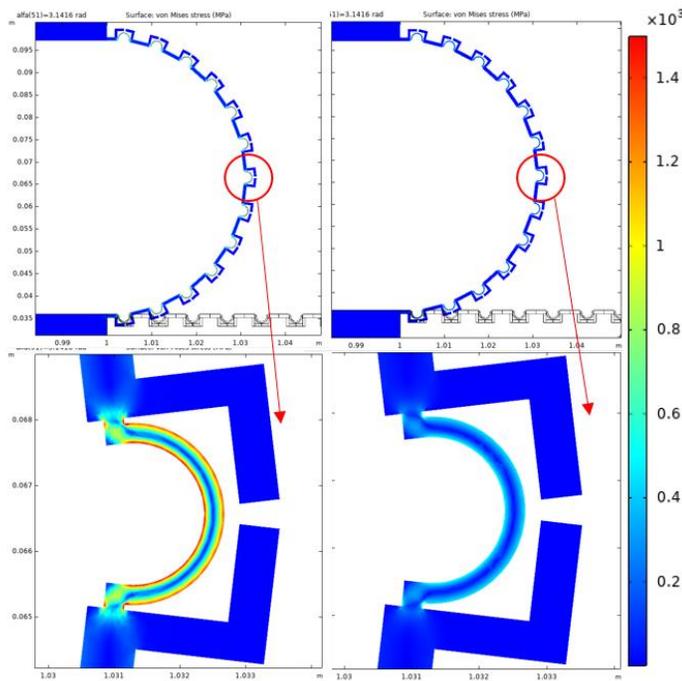The stress distribution of the middle cell where the stress is measured is shown in Figure 8.

FIGURE 8: DEFORMATION OF THE COMPLIANT ARRAYS MADE OF 13 CELLS (N=13) Φ=180 DEGREES AND STRESS DISTRIBUTION IN THE MIDDLE CELL OF THE ARRAY FOR ANGLE Φ=180 DEGREES FOR THE DIFFERENT MATERIALS, STEEL (LEFT) AND SUPERELASTIC NITI (RIGHT)

All of the stresses are represented on the same scale with maximum of 1500 MPa. It is notable that for a complete fold the deformation of a single cell is the same for both of the materials. The difference as discussed are the stresses which can be seen on the closer image of the cell. Therefore, by combining effort of the geometric and material nonlinearity, the structure made from Nitinol could have larger dimensions and higher stability while maintaining low stresses.

4. DESIGN OF METAMATERIAL COMPLIANT JOINTS

The design of the arc is most important in determining the performance of the entire structure. As noted in Figure 8, the maximum stresses are expected in this part. Hence the arc geometry is combined to form a metamaterial, as shown in Figure 9. These metamaterials can be built with n-number of arcs on the lower part of the row, and m number of rows.
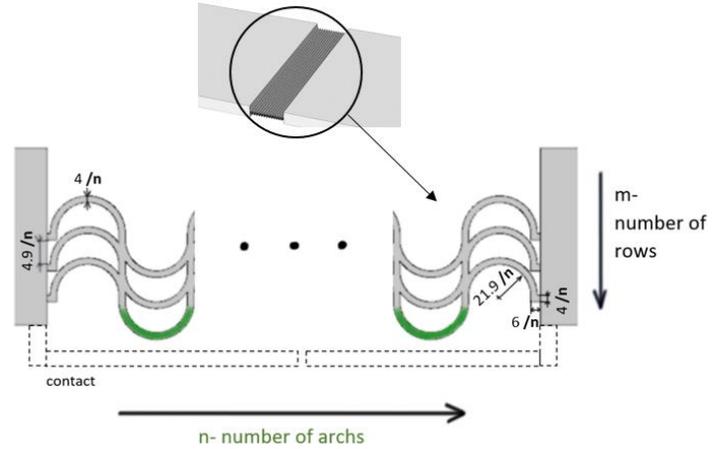

FIGURE 9: METAMATERIALS BASED ON COMPLIANT ARRAYS

All of the dimensions are parametric in order to fit a metamaterial structure with n-number of arcs in the area of the hinge with dimensions 100 mm x 36 mm. The first row is always in the middle of the hinge in the vertical direction. All of the other m -1 number of rows are offset from the first row for 4.9/n mm. For maintaining the nonlinear stiffness an additional contact surface could be added which is shown in Figure 9 with dotted lines.

In Figure 10 the maximum stress in the middle cell for different numbers of arcs (n) and one row (m=1) with the steel material is shown. Also with this geometry the increase of number of arcs improves the performance of the hinge. It is also notable that for the same number of arcs and the same material, the performance of these kind of structures is better than the compliant arrays introduced previously. For example in the case for the steel compliant array made of 9 cells (Figure 6) the stress surpasses the stress constraint for a complete fold whereas the case with the metamaterial with a single row with 9 arcs the complete fold is achieved with stress almost three times lower than the stress constraint as shown in Figure 10. This result is mainly attributed to the dimensions of the arc, which all but the thickness are different for the different geometries presented, .
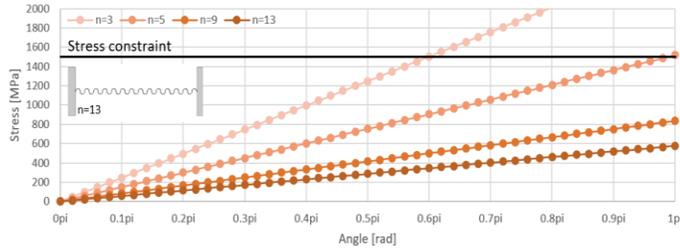
FIGURE 10: MAXIMUM VON MISES STRESS ON THE MIDDLE CELL FOR THE METAMATERIALS WITH DIFFERENT NUMBER OF ARCS (N) AND ONE ROW (M=1) WITH THE STEEL AISI 4340

The new metamaterial geometry has better performance than the compliant arrays made of steel, but not the superelastic compliant arrays. In Figure 11 the maximum stress measured in the middle arc for the NiTi metamaterial with one row (m=1) is shown. The benefit of the superelastic material is apparent . When compared to the same designs made of steel the stresses are drastically decreased. The stresses for this design are so low that the materials does not even enter the superelastic region of the stress-strain curve. For the same material the metamaterial geometry has better performance than the compliant arrays discussed before. For example the metamaterial with one row (m=1) and compliant array n=3 are compared. They both have the same arc thickness of 1.33 mm. However the compliant array enters the superelastic region since the stresses are much higher than in the case of the metamaterial built for the same number of arcs (n=3).
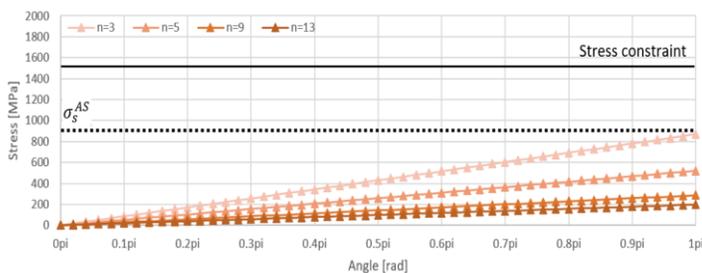

FIGURE 11: MAXIMUM VON MISES STRESS IN THE MIDDLE CELL FOR THE METAMATERIALS WITH DIFFERENT NUMBER OF ARCS (N) AND ONE ROW (M=1) WITH THE NITI MATERIAL

The case when the number of rows is increased, with 13 arcs (n=13) for the steel material is shown in Figure 12. The stress is measured in the middle cell of the first row, which is always in the same position, in the middle of the hinge in the vertical direction. Here the case with a single row is included as well. The number of rows (m) has an opposite impact on the performance of the hinge than the number of arcs (n). Even though on the plot shown in Figure 12 the metamaterial with one row has the lowest stress for

the complete fold, the metamaterial with two rows (m=2) and 13 arcs (n=13) has a better performance than the metamaterial with one row (m=1) and three arcs shown (n=3) in Figure 10 for the same steel material. The number of rows of the metamaterial increases the stiffness of the whole structure. Even though the joint should be flexible in order to achieve the complete fold of 180 degrees, the stiffness should not be too to ensure stability of the whole structure.
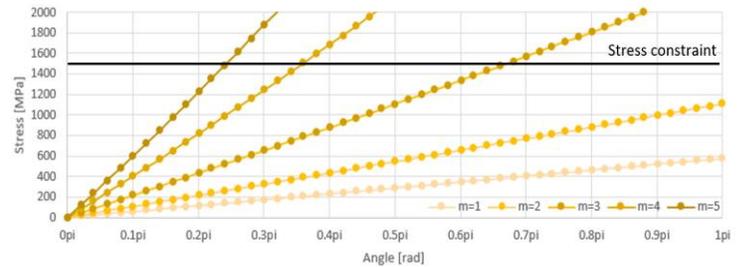

FIGURE 12: MAXIMUM VON MISES STRESS IN THE MIDDLE CELL OF THE FIRST ROW (M=1) FOR THE METAMATERIALS WITH 13 ARCS (N=13) AND DIFFERENT NUMBER OF ROWS WITH THE STEEL AISI 4340

The case for different numbers of rows and 13 arcs (n=13) with the superelastic Nitinol is shown in Figure 13. As before the stresses are drastically decreased compared to the designs with the steel material. Considering the importance of having more rows for stability, if the more flexible material is used even the geometry with three rows has lower stresses than the geometry with two rows with the steel. Additionally the superelasticity allows good performance even in the case of 5 rows.
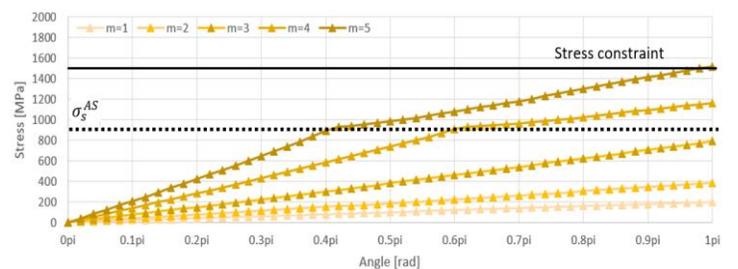

FIGURE 13: MAXIMUM VON MISES STRESS IN THE MIDDLE CELL OF THE FIRST ROW (M=1) FOR THE METAMATERIALS WITH 13 ARCS (N=13) AND DIFFERENT NUMBER OF ROWS WITH THE NITI MATERIAL

The stress distribution for the metamaterials with different number of rows for the complete fold and the steel material are shown in Figure 14. The scale of the color in the plots is fixed at 1500 MPa which is the stress constraint in the analysis. A pattern in the distribution of the maximum stresses can be seen. The

regions with maximum stresses are further from the middle line of the whole structure and the arcs with maximum stresses repeat periodically.
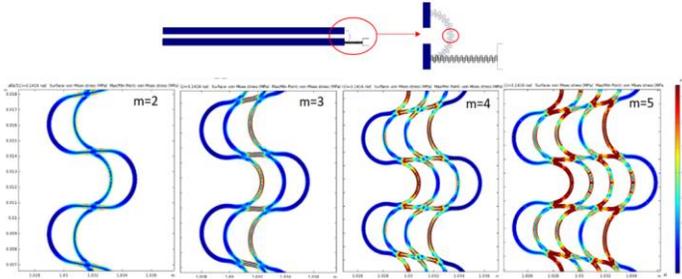

FIGURE 14: STRESS DISTRIBUTION IN THE MIDDLE OF THE DIFFERENT METAMATERIALS BUILT WITH DIFFERENT NUMBER OF ROWS FOR ANGLE Φ=180 DEGREES AND THE STEEL MATERIAL

The stress distribution of the same geometries made of Nitinol is shown in Figure 15. Here the benefit of the superelasticity is also visible since the stresses are much lower. The pattern of the distribution of the stress previously mentioned is the same regardless the materials applied.
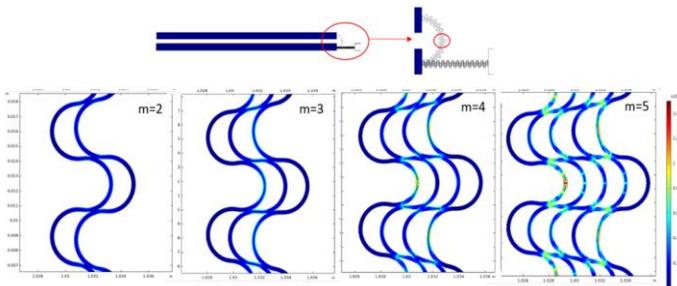

FIGURE 15: STRESS DISTRIBUTION IN THE MIDDLE OF THE DIFFERENT METAMATERIALS BUILT WITH DIFFERENT NUMBER OF ROWS FOR ANGLE Φ=180 DEGREES AND THE SUPERELASTIC NITINOL

In Figure 16 a metamaterial with an alternative geometry is shown. In this geometry the array that is being repeated consists of two rows of the metamaterial. The first row is always positioned in the middle of the hinge in the vertical direction. The second row is mirrored around its symmetry axis and it is moved in the vertical direction in a way that the intersection of the two arcs is equal to the thickness of the arc. This structure can be repeated i-times; the cases for i = 1 and 2 are shown in Figure 16. The model of the metamaterial used here has 13 arcs (n=13).
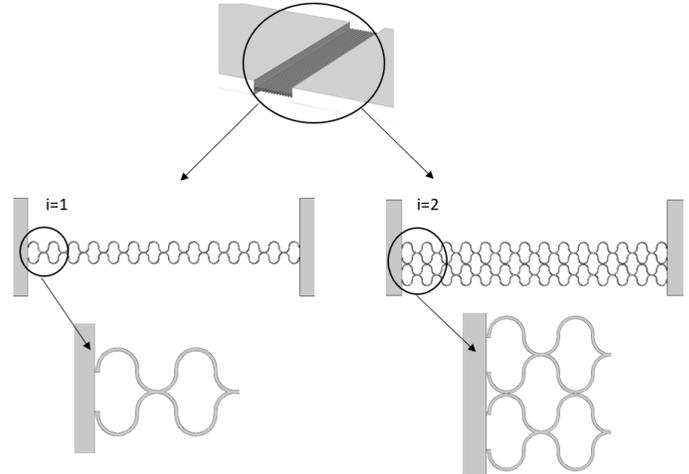

FIGURE 16: ALTERNATIVE METAMATERIAL GEOMETRY WITH ONE AND TWO ROWS

In Figure 17 the maximum stress in the middle cell of the metamaterial with one and two rows with the steel material is shown. Similar to the metamaterials presented before, increasing the number of rows increases the stresses in the hinge. In the case for one row (i=1) it is notable that the deflection of the joint at the stress constraint is around 0.4π. This structure is similar to the metamaterial with 13 arcs (n=13) and two rows (m=2). In Figure 12 this joint achieves the complete fold with stresses below the stress constraint.
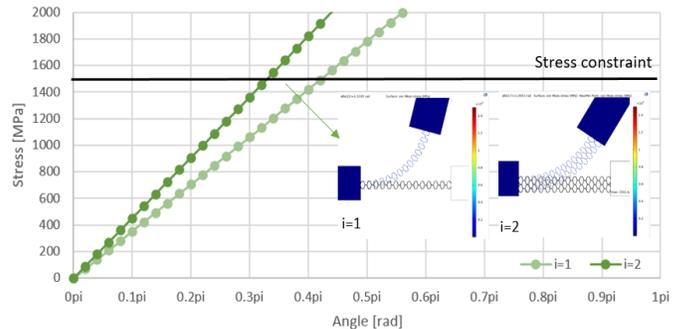

FIGURE 17: MAXIMUM VON MISES STRESS IN THE MIDDLE CELL OF THE FIRST ROW WITH THE STEEL MATERIAL

In Figure 18 the maximum stress in the middle cell is presented. These results are for the alternative metamaterials built with one and two rows (i=1,2) made of superelastic Nitinol. As before, the Nitinol is beneficial since both of the geometries achieve the complete fold while the maximum stresses in the middle cells are below the stress constraint. Here as well the geometry with the higher number of rows has higher stresses. The geometry with i=1 can be compared with the metamaterial with two rows (m=2). In Figure 13 this structure with Nitinol has

7

stress of 400 MPa for the complete fold. On the contrary the geometry shown in Figure 18 has stress of around 1000 MPa for the complete fold, which is around 2.5 times higher.
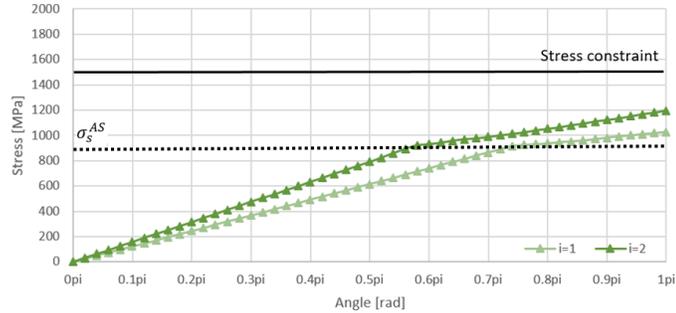

FIGURE 18: MAXIMUM VON MISES STRESS IN THE MIDDLE CELL OF THE FIRST ROW WITH THE NITI MATERIAL

Figure 19 shows the stress distribution of the middle cells for a complete fold. It is noticeable that for different number of rows (i) not only are the stress levels different, but also the stress distribution is different and the maximum stresses are not located in the same regions. The geometry with two rows (i=2) has more regions where the stresses are high, whereas the geometry with one row (i=1) has only one region with high stresses, located where the two arcs are bonded.
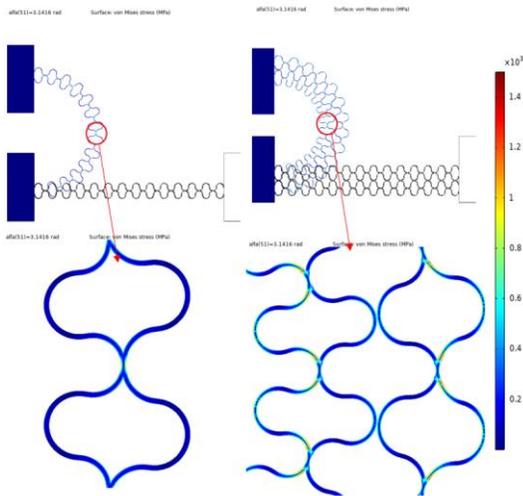

FIGURE 19: STRESS DISTRIBUTION IN THE MIDDLE CELL OF THE FIRST ROW WITH THE NITI MATERIAL

5. COMPARATIVE ANALYSIS

A comparison of the performance among the different designs analyzed in this paper is based on the volume of the hinge. All of the chosen geometries have roughly same volumes compared to the total volume of the hinge space. The reference for the choice was the alternative metamaterial design with two rows (i=2). The designs with the same volume from the other geometries are the case with 9 cells (n=9) for the compliant arrays and the metamaterial design with n=13 and m=4. Three main parameters were chosen for the comparison, the maximum stress in the middle cell, the actuation moment and the rotational stiffness for a fold of 180 degrees. According to Daams (1994) in [21] the average maximum push force that both male and female in functional posture can exert at shoulder height is 211 N. Since the length of the side panel is 1m, the average maximum actuation moment would be 211 Nm, indicated on Figure 20 with a hand symbol. All of the designs are made of the superelastic Nitinol and the results are for the complete fold of 180 degrees. The results are shown in Figure 20. The compliant array has the lowest maximum stress in the middle cell and the lowest needed actuation moment to achieve the complete fold. As shown the metamaterials, both regular and the alternative design have almost the same maximum stress, whereas the regular metamaterial needs lower actuation moment for the complete fold. Since very low stiffness would also mean lower stability of the whole structure, this parameter is also very important. Even though the compliant array has lower stress and actuation moment, the stiffness is also much lower than the metamaterials. Since the stresses for the metamaterials are lower than the stress constraint and the actuation moment is lower than the moment achieved by a human hand the compliant array has lower overall performance than the metamaterials. The choice between the different geometries must take into account several design requirements. Considering all the factors, the alterative metamaterial has the best performance of all of the geometries.
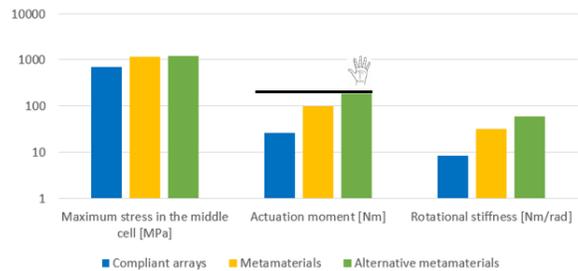
FIGURE 20: COMPARISON BETWEEN THE DIFFERENT GEOMETRIES MADE OF SUPERELASTIC NITINOL FOR DEFORMATION OF 180 DEGREES

The potential application of the designed compliant joint to a shipping container is shown in Figure 21. The joints are assumed to be made of the alternative metamaterial and are positioned in the vertical direction which enables the folding of the container. One possibility for the folding of the container is shown in Figure 21 where only the upper and lower walls of the container are

folded. Due to the application of the compliant joints, the container is flexible and it can be fitted in different spaces. This would be beneficial in the transport of the containers on ships or trucks since there are many possibilities for their positioning and required sizes.
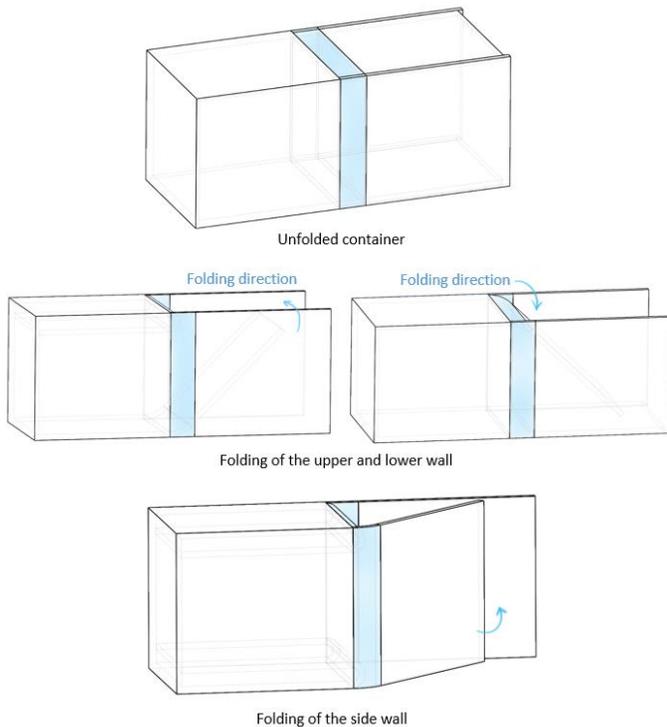

FIGURE 21: DIFFERENT CONFIGURATIONS OF THE SAME SHIPPING CONTAINER ACCORDING THE ACTIVATED HINGES

6. CONCLUSIONS

In the paper compliant joints were proposed for a reconfigurable container requiring a complete fold of 180 degrees. The compliant arrays show great potential in achieving a complete fold while maintaining the stresses under the specified stress constraint of 1500 MPa. With the increase of the number of cells in the arrays the performance is better. This trend is the same for the metamaterials which provide stability of the whole structure due to the increased number of rows while still satisfying the stress constraint. The ability to design metamaterials with more rows, from stiffer materials like the steel while still maintaining the complete fold shows that these kind of structures have great potential. The combined effort of the geometry and the material is also very important, since the superelasticity of NiTi was proven to be crucial in lowering the measured stresses.

When these compliant joints are applied to a shipping container in the hinge space, a foldable container can be constructed. The compliant hinges can be located in different places and they can be foldable in the vertical and/or in the horizontal direction. By varying the number and the position of the hinges, and by selective actuation different configurations could be achieved. With these flexible hinges the geometry of the whole container can be configured according to the needs. In the comparative analysis the cost of the material and/or production, including logistics of the transport of these kind of containers with various sizes. was not taken into consideration .Future work includes formal optimization of the geometry and material to achieve a complete fold, while having stresses as low as possible and having suitable stability of the hinge and the whole structure.

REFERENCES

[1] Sun, J., Guan, Q., Liu, Y. and Leng, J., 2016. Morphing aircraft based on smart materials and structures: A state-of-the-art review. *Journal of Intelligent material systems and structures*, *27*(17), pp.2289-2312.

[2] Ferraro, S. and Pellegrino, S., 2018. Self-Deployable Joints for Ultra-Light Space Structures. In *2018 AIAA Spacecraft Structures Conference* (p. 0694).

[3] Floreano, D., Mintchev, S. and Shintake, J., 2017, May. Foldable drones: from biology to technology. In *Bioinspiration, Biomimetics, and Bioreplication 2017* (Vol. 10162, p. 1016203). International Society for Optics and Photonics.

[4] Chai, T.J. and Tan, C.S., 2019, January. Review on deployable structure. In *IOP Conference Series: Earth and Environmental Science* (Vol. 220, No. 1, p. 012034). IOP Publishing.

[5] Fenci, G.E. and Currie, N.G., 2017. Deployable structures classification: A review. *International Journal of Space Structures*, *32*(2), pp.112-130.

[6] Doroftei, I.A., Bujoreanu, C. and Doroftei, I., 2018, November. An Overview on the Applications of Mechanisms in Architecture. Part II: Foldable Plate Structures. In *IOP Conference Series: Materials Science and Engineering* (Vol. 444, No. 5, p. 052019). IOP Publishing.

[7] Bowen, L., Frecker, M., Simpson, T.W. and Strzelec, R., 2017, January. A Framework for the Design and Optimization of Self-Folding Structures. In *ASME 2017 International Design Engineering Technical Conferences and Computers and Information in Engineering Conference*. American Society of Mechanical Engineers Digital Collection.

[8] Butler, J., Bowen, L., Wilcox, E., Shrager, A., Frecker, M.I., von Lockette, P., Simpson, T.W., Lang, R.J., Howell, L.L. and Magleby, S.P., 2018. A model for multi-input mechanical advantage in origami-based mechanisms. *Journal of Mechanisms and Robotics*, *10*(6).

[9] Jovanova, J. and Frecker, M., 2017, September. Two Stage Design of Compliant Mechanisms With Superelastic Compliant Joints. In ASME 2017 Conference on Smart

Materials, Adaptive Structures and Intelligent Systems (pp. V002T03A019-V002T03A019). American Society of Mechanical Engineers.

[10] Jovanova, J., Domazetovska, S. and Frecker, M., 2018, January. Modeling of the Interface of Functionally Graded Superelastic Zones in Compliant Deployable Structures. In *ASME 2018 Conference on Smart Materials, Adaptive Structures and Intelligent Systems*. American Society of Mechanical Engineers Digital Collection.

[11] Jovanova, J., Frecker, M., Hamilton, R.F. & Palmer, T.A. 2017, "Target shape optimization of functionally graded shape memory alloy compliant mechanisms", Journal of Intelligent Material Systems and Structures, pp. 1045389.

[12] Tummala, Y., Frecker, M.I., Wissa, A.A. and Hubbard Jr, J.E., 2013. Design and optimization of a bend-and-sweep compliant mechanism. *Smart materials and structures*, *22*(9), p.094019.

[13] Calogero, J.P., Frecker, M.I., Hasnain, Z. and Hubbard Jr, J.E., 2016. A dynamic spar numerical model for passive shape change. *Smart Materials and Structures*, *25*(10), p.104006.

[14] Calogero, J.P., Frecker, M.I., Hasnain, Z. and Hubbard Jr, J.E., 2018. Dual Optimization of Contact-Aided Compliant Mechanisms for Passive Dynamic Shape Change. *AIAA journal*, *56*(9), pp.3745-3756.

[15] Konings, R. and Thijs, R., 2001. Foldable containers: a new perspective on reducing container-repositioning costs. *European journal of transport and infrastructure research*, *1*(4).

[16] Lee, S. and Moon, I., 2020. Robust empty container repositioning considering foldable containers. *European Journal of Operational Research*, *280*(3), pp.909-925.

[17] Auricchio F., Taylor R. L., Lubliner J., 1997, "Shape-memory alloys: macromodeling and numerical simulations of the superelastic Behavior," Computational Methods in Applied Mechanical

[18] Hamilton, R.F., Palmer, T.A. and Bimber, B.A., 2015. Spatial characterization of the thermal-induced phase transformation throughout as-deposited additive manufactured NiTi bulk builds. Scripta Materialia, 101, pp.56-59.

[19] Bimber, B.A., Hamilton, R.F., Keist, J. and Palmer, T.A., 2016. Anisotropic microstructure and superelasticity of additive manufactured NiTi alloy bulk builds using laser directed energy deposition. Materials Science and Engineering: A, 674, pp.125-134.

[20] Venkiteswaran, V.K. and Su, H.J., 2016. Pseudo-rigid-body models for circular beams under combined tip loads. *Mechanism and Machine Theory*, *106*, pp.80-93.

[21] Karwowski, W. ed., 2006. International Encyclopedia of Ergonomics and Human Factors, -3 Volume Set. Crc Press.